Journal of Undergraduate Chemistry Research, **2021**,20 (3), 49

CHARACTERIZING MICROPLASTIC DEGRADATION IN A SIMULATED MARINE ENVIRONMENT

Xiaoxiao Wang*, Rachel Shubella*, Evan Ammidown*, Heather C. S. Chenette†

Chemical Engineering Department, Rose-Hulman Institute of Technology, Terre Haute, IN 47803

Abstract

This study establishes and implements characterization methods to investigate the potentially hazardous degradation products of plastics found floating on the ocean surface. Unprocessed plastic pellets (polyethylene, polypropylene, and polystyrene) and consumer drinking straw pieces (non-biodegradable straws and compostable straws) were placed in simulated seawater and examined for one year. Analyses were performed to study the effects of ultraviolet light and physical mixing on the degradation including yellowness index (YI), pellet mass loss, SEM, ATR-FTIR, and GCMS using an original extraction technique. Changes in YI ranged from 11 ± 3 to 36 ± 9, suggesting photooxidation occurred. SEM images show indentations and surface smoothening of all samples. FTIR results yielded carbonyl indices ranging from 1.81 to 1.93. Degradation products were isolated from the simulated seawater solution using a novel extraction process and identified by GCMS showing aliphatic hydrocarbons for PE and PP, whereas those of PS are cyclic aromatic compounds.

†*Corresponding author:* chenette@rose-hulman.edu

Key words: *polymer chemistry, degradation products, extraction, biodegradable plastics*

Introduction

With an increasing amount of plastics entering the ocean, plastics pose severe threats to marine ecology. It is estimated that between 4.8 and 12.7 million tons of plastic enters the ocean every year[1]. At least 267 species, including seabirds and marine mammals, have been reported to be influenced by plastic, either becoming trapped in plastics, or mistakenly consuming plastic bags as food[2,3]. The impacts on birds, fish, and turtles due to ingestion of and entanglement in plastic products can not only be lethal to individual animals, but the impacts are also global, and occur at a high frequency. Plastics pollution is a stressor, which can act in parallel with other stressors such as ocean temperature changes, ocean acidification, and the over exploitation of marine resources, leading to a dramatic shift in the ecology of marine systems[4].

Because of plastics' durable properties, the degradation process is very slow. Plastic degradation occurs either abiotically (i.e., thermally, hydrolytically, or by UV-light) or biotically (i.e., by microorganisms). Studying abiotic degradation is important even in the context of a marine environment where one might expect biotic degradation to be prevalent. As observed by Syranidou, et al., abiotic degradation can stimulate biodegradation because the formation of carbonyls on the surface encourages the breakdown of higher molecular weight compounds to smaller ones. They observed that abiotic conditions, such as UV radiation, promote degradation of plastics with a carbon-carbon backbone, and thereby increase the likelihood for biodegradation to take place[5]. In the ocean, most degradation is photoinitiated by sunlight, with the first visible sign of plastic degradation being color change. The tertiary carbon on the backbone of polypropylene makes it more prone to produce free radicals. Polypropylene, therefore, has a lower activation energy for photodegradation than polyethylene and degrades more quickly. Polystyrene degrades faster than both due to the phenyl group on the tertiary carbon[6].

Studying plastic waste degradation in the environment continues to be relevant to better understand the relationship to microplastic and nanoplastic formation. Microplastics, classified by the U.S. National Oceanic and Atmospheric Administration (NOAA) as less than 5 mm in diameter, make a large proportion among the debris[7]. Microplastics can come from either a primary source (i.e., microbeads used to produce personal care products), or a secondary source (i.e., fragments from degradation of larger plastics). Recent publications have suggested that microplastics will subsequently degrade into nano-sized plastic particles. While they have no official size definition, studies like those conducted by El Hadri, et al., often categorize nanoplastics as particles in the range of 1 nm to 1 μm, in part because of the large environmental effect associated with this small size. As they observed, nanoplastics may have a greater impact than microplastics due to their dimensions and colloidal behavior; their smaller size makes tissue penetration and accumulation in organs a possibility[8].

Studies on chemicals released by plastics under UV exposure in a simulated beach environment (only mechanical abrasion) and aqueous conditions have been performed previously[9,10]. However, currently there are limited studies on the simulated ocean surface environment, and no studies regarding the toxicity of the microplastics have been performed[11,12]. Furthermore, although the thermal degradation products and rheological properties of different plastics are widely known, the potential organic byproducts from UV degradation in a simulated seawater environment have been seldom studied[10]. Finally, there are a variety of studies predicting the long-term effects of plastic degradation including microplastic and nanoplastic formation. Yet, the potential hazards posed by plastic after just one to two years of UV exposure is unknown[7]. The goal of this study was to investigate the degradation mechanism of plastics being exposed to short-term weathering conditions that mimic an aqueous marine environment.

The plastic materials chosen for this study were three plastic pellets, low density polyethylene (PE), homopolymer polypropylene (PP), general purpose polystyrene (PS), and two consumer plastics, non-biodegradable straws and compostable straws. These plastics account for 74% of global plastic production[13], and all have densities lower than that of seawater (1030 kg/m3), so they will float on the ocean surface[14]. The extent of degradation was

analyzed by looking at pellet mass loss and ASTM D1925 yellowness index (YI) using CIE 1931 XYZ color space. The degradation products were characterized via gas chromatography mass spectroscopy (GCMS), and images and data on changes in the physical and chemical properties of the plastic were collected using scanning electron microscopy (SEM) and attenuated total reflectance Fourier transform infrared spectroscopy (ATR-FTIR).

Experimental Methods

Samples and experimental setting

The experiment was designed to investigate the degradation behavior of plastics in a simulated ocean environment. The pH of simulated seawater (35 g/L NaCl) was adjusted to 7.0 (±0.5) by HCl. The three types of plastic resins used in the experiment were low density polyethylene (PE) (Chevron Phillips Chemical Company, USA), homopolymer polypropylene (PP) (Flint Hills Resources, USA), and general purpose polystyrene (PS) (Resirene, USA). All plastics were in pellet form, approximately 0.4 ±0.1 cm in diameter, and contained little to no stabilizer. The melt index for PE, PP and PS are 7, 12, 16 g/10 min, respectively. The non-biodegradable straws, made of PP, were obtained from a cafe in Terre Haute, Indiana. The compostable straws (Eco-Products, USA), were purchased from Amazon. Both kinds of straws were cut into 0.5 cm pieces.

Three different pellet concentrations per simulated seawater volume were used: 10 mg/mL, 20 mg/mL, and 30 mg/mL for each of PE, PP and PS. While likely higher than typical concentrations found in real conditions, these concentrations are in range of a similar literature study.[11] For non-biodegradable and compostable straws, a concentration of 20 mg/mL was used. These were placed into separate glass jars (200 mL). Simulated ocean water (35 g/L NaCl, 150 mL) was added to each jar. The setup included 20 total jars with duplicate samples for each polymer. The samples were placed on a shaker table (Excella E24, New Brunswick Scientific, USA) coupled with a UV-AB lamp (302 nm, 3 mW/cm^2, VWR, USA). Photographs of the shaker table and sample jars can be seen in Figures 1 and 2. The shaker table was set to 120 rpm, and jars were rotated every 2 weeks to ensure equal UV exposure. The jars were not covered with a lid, and were therefore refilled to the starting volume every two weeks with deionized water. The UV exposure and mixing were continuous (24 hours a day) during the one-year time span. In a real environment, plastics would have approximately 12 hours of UV exposure. This means one year of UV exposure in the experimental environment would be approximately equivalent to two years of UV exposure in a real environment.

YI Color Analysis

Approximately 60 post-oven dried pieces of unexposed and exposed PP, PE, and PS were placed on a paper towel to be photographed. To observe visual changes in the samples, photographs were taken under proper lighting using a high-resolution digital camera (12 megapixel). The angle between the camera lens axis and the lighting source axis was approximately 45° because the diffuse reflection responsible for color occurs at 45° from the incident light[15]. The distance from the bottom of the camera lens to the plastic was 20.5 cm, and images were taken in focus with no flash and daylight conditions. The masses of exposed and unexposed pellets were also investigated to observe any effects of mechanical abrasion which could yield a higher YI.

Once the color images of the plastics were captured, the color was analyzed quantitatively using Microsoft Office Logo Color Palette with RGB codes. By utilizing the grid feature, a computer pointer was placed at a grid point along the x-axis or y-axis, and a set of RGB values corresponding to that pixel of the grid point were obtained from the Eyedropper tool, with the origin located at the center of a plastic sample[16]. A random pellet with no shadows was selected from each image, and ten RGB sets of values were obtained across that pellet of unexposed and exposed PP, PE, PS, and of non-biodegradable straws, and compostable straws. Each set of RGB values was converted to CIE 1931 XYZ[16,17]. The ASTM D1925 yellowness index was then computed for each value to analyze the degree of degradation (Equation 1).

$$YI_{D1925} = \frac{100(1.28X - 1.062Z)}{Y} \quad (1)$$

where X, Y, and Z are the CIE Tristimulus values/2° observer. Equation 1 has a positive value to a yellowish object, but negative value to a bluish object. Therefore, a negative YI is not measuring yellowness.

SEM Analysis

SEM images of the center of the pellets were collected to capture changes in the surface texture of plastic pellets. Three pellets

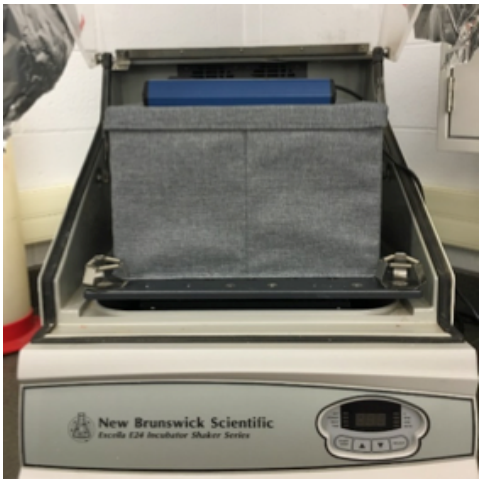

Figure 1. Shaker table showing box containing samples and UV light placement atop box

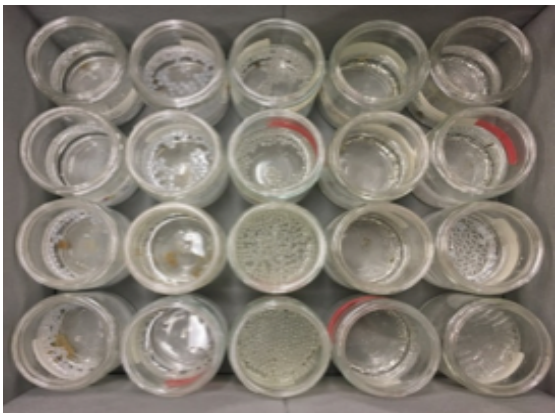

Figure 2. Open sample jars contained in box

from each type of plastic, both unexposed and exposed to degradation conditions, were randomly selected to be analyzed by scanning electron microscopy (SEM) on a HITACHI TM3000 microscope. Those collected after 11 months of UV degradation were washed by deionized water and dried with a Kimwipe. Gold sputtering was considered, but after reasonably detailed images of pellet surfaces were obtained without it, the technique was not used for any samples. All samples were run at 5kV accelerating voltage, with magnifications of 300-4,000x. No additional measures were taken to mitigate charging.

FTIR analysis

An FTIR spectrometer (Cary 630, Agilent Technologies, USA), equipped with an attenuated total reflectance (ATR) diamond crystal attachment, was used for analysis. Pellets were heated at 350°C for 10 minutes, then pressured to plastic sheets in a hydraulic press (Harco Industries, USA) under 5000 psi. Three pellets from a given type of plastic and experimental condition were randomly selected for analysis. The carbonyl index (CI) was used to determine the degree of degradation[18]. The main chemical groups seen in the photochemical oxidation of polymers include carbonyl and hydroxyl groups. Since the carbonyl absorption band has a constant position, high intensity, and freedom from other interfering bands in the 1540-1800 cm^{-1} region of the IR spectra, it is ideal for the observation of photodegradation. The reference bands used for PE, PS, and the non-biodegradable straws were the symmetric methylene stretching band at 2850 cm^{-1} (Equation 2), and

$$CI_{PS,PE,nonbiodeg} = \frac{Abs(1700 - 1760\ cm^{-1})}{Abs(2850\ cm^{-1})} \quad (2)$$

for PP was the methyl rocking band around 972 cm^{-1} (Equation 3).

$$CI_{PP} = \frac{Abs(1700 - 1760\ cm^{-1})}{Abs(972\ cm^{-1})} \quad (3)$$

Linear baseline corrections proposed by Mylläri et al. were applied since the baselines will shift during photodegradation.

GCMS Analysis

A novel extraction method was developed to recover organic degradation products from the saltwater solutions. After 11 months of exposure, random 15 mL aliquots of saltwater solutions were taken from each wide-mouth jar and placed in a 20 mL scintillation vial. No pellets were removed when these aliquots were taken. 1-2 drops of 1 M HCl were added to each vial in order to protonate the organics in solution. Approximately 1 mL of hexane was added to each vial, and the solution was sonicated in order to allow the organics to partition into the hexane. A separatory funnel was then used to separate the hexane layer from the saltwater layer, and the hexane was pipetted into an HPLC vial.

A GCMS (GCMS-QP2010S, Shimadzu, USA) in splitless mode with a 30.0 m capillary column (Elite 5MS) was used for analysis. The temperature program used for analysis included a column temperature of 60°C, injection temperature of 350°C, and flow rate of 15 mL/min. The GCMS was rinsed with methanol between runs to ensure the column was free of impurities. One measurement required approximately 30 minutes. To verify the novel extraction technique, a 0.01M solution of benzoic acid in prepared salt water was extracted according to this protocol. The GCMS spectra of the extract confirmed presence of benzoic acid (99% match with library database).

Results and Discussion

YI Color Results

Since plastic are organically based, exposure to UV radiation causes them to change color, crack, break, and shatter. Yellowing in plastics occurs from chemical interactions that oxidatively transform a compound, leading to new conjugated structures, and is therefore a measure of the degree of degradation.The ASTM D1925 yellowness index of three types of exposed and unexposed plastic pellets and two types of exposed and unexposed straws were computed using CIE 1931 XYZ color space (Table 1, Figure 3, Figure 4)

Table 1: Average ASTM D1925 yellowness index for all unexposed and samples exposed to UV light for one year with relative standard deviation

Plastic Type	YI for Unexposed Samples ±Stdev	ASTM D1925 Yellowness Index ±Stdev
PE	9 ± 3	11 ± 3
PP	12 ± 2	25 ± 5
PS	7 ± 2	36 ± 9
Non-biodegradable straws	10 ± 1	13± 2
Compostable straws	13 ± 2	19± 3

Figure 3. Spread of ASTM D1925 yellowness index for all unexposed samples

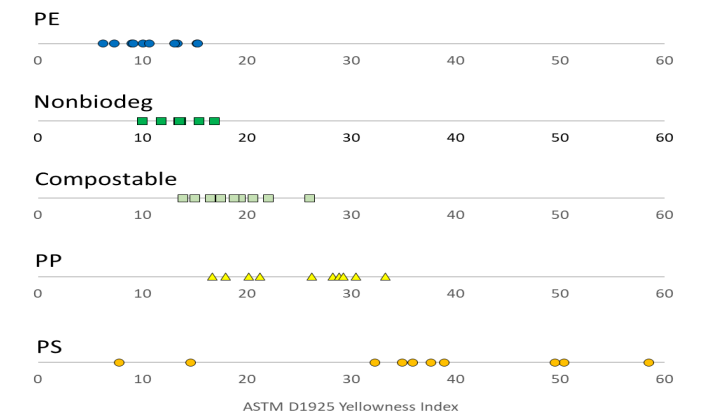

Figure 4. Spread of ASTM D1925 yellowness index for all exposed samples to UV light for one year

From Figure 3, it can be seen all plastic samples have some initial degree of yellowness. However, from Figure 4, it can be observed the yellowness indices increased for all samples, especially for PP and PS, after one year of UV exposure. Yousif et al. reported a YI of –8.66 for additive-free PE and 4.35 for additive-free PP after one month of UV exposure[19]. The YI values after one-year of UV exposure follow the same trends, with the YI of PE being significantly smaller than that of PP. An increase in YI values is expected because photooxidation exposure causes degradation of some of the single bonds in the polymer, which leads to new conjugated structures after reaction with oxygen and a propagation reaction. In turn, these new structures absorb some of the shorter wavelengths of light, which cause the yellow appearance. Therefore, yellowing worsens over time as total degraded polymer increases[19].

Overall, PS exhibits a high degree of yellowness compared to other plastic samples. This is attributed to the accumulation of conjugated bond sequences in the polymer backbone. PS is produced by radical-initiated polymerization which Callister and Rethwisch observed makes it easier to undergo bond scission, chain crosslinking, and oxidative degradation. Furthermore, they saw that several impurities and irregularities in PS, including hydroperoxides, aromatic carbonyl groups, olefin bonds, chain peroxide linkages, and ketonic impurities absorb the light of wavelengths longer than 300 nm. On the other hand, the authors saw that it takes longer for PE and PP to form conjugated polyenes because of their crystallinity. Since there are more amorphous regions in PP than in PE, it degrades at a faster rate, which is why its YI is higher[20].

The PP, PE, and PS samples are all additive-free, while the non-biodegradable straws have plasticizers, antioxidants, ultraviolet light filters, and inert fillers. These additives help keep the straws from cracking, reduce harmful interactions between the plastic and oxygen in the air, and shield the plastic from the effects of sunlight to prevent radiation from adversely affecting the plastic[19]. Hence, the YI of the non-biodegradable straws is lower than that of additive-free PP. Known examples of utilizing digital imaging to perform YI analysis in literature are rare [16,21,22], and at the time of this writing the authors know of no prior studies that use this method to analyze plastic degradation. While it is not a replacement for sophisticated color measurements, and the YI values cannot be directly compared to others from literature without proper calibration of the respective systems, it is an attractive alternative due to its simplicity, versatility, and low cost.

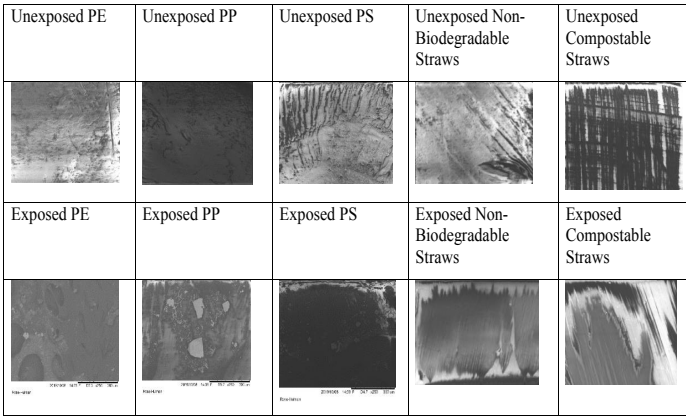

Figure 5. SEM images for surfaces of unexposed and exposed plastic samples under 11 months UV exposure.

The pellet mass loss was also investigated to observe the relationship between mass loss and YI. It was found the uncertainty in the measured mass losses was larger than the percent mass loss, which ranged from 0-3%. Because polymers require a substantial amount of time to degrade, it is hypothesized one-year exposure time is not enough to observe losses in mass given the sensitivity of the experimental setup. It should be noted that unless a more robust drying method is used, the associated hydrolysis may offset the mass loss to some degree.

Changes in surface texture

SEM images were taken of the surface of three types of plastic pellets and two types of straws both before (unexposed) and after 11 months exposure (exposed) to UV light (Figure 5).

It was expected that the surfaces of all samples would show signs of degradation, potentially smoothening of the pellet surface or the formation of large craters where noticeable pieces of the surface have been removed. The PE sample shows both features. First, the surface appears smoother after exposure, indicated by the loss of the bright white patterning seen in the unexposed image. The lack of contrast indicates a more uniform surface height for most of the pellet's surface. Additionally, the PE image taken after 11 months exposure shows indentations (approx. 180 x 70 μm) on the surface, indicating some loss of surface mass. This phenomenon is expected as the surface bonds weaken from UV exposure and physical mixing may also promote breakage at the pellet surface.

The PP images also show the same trends. The 11 month PS image shows large dark areas, indicating these parts of the surface are at a greater depth compared to the lighter areas (i.e. these areas of the surface are lower than others). The 11 month PS sample shows surface smoothing, as it lacks the high contrast pattern seen in the unexposed image. Also observed in the exposed PS sample are cubic crystals which are likely residual salt not sufficiently removed after rinsing.

Both straw samples show some degree of surface change. Both unexposed straw samples show clear patterning, indicated by the varying degrees of whites, grays, and black in proximity. Both exposed samples exhibit a more uniform surface, but the degree to which they changed is difficult to quantify.

It should be noted that conclusions drawn from the SEM images are qualitative in nature. Contrast differences, as well as light/dark features in the images may be influenced by sample charging, location differences between samples, as well as the differences between randomly chosen samples for imaging. Considering these limitations, while surface changes to the samples seem to indicate visual signs of degradation, we cannot draw strong conclusions from these images

Changes in FTIR spectra

The PP, PE, and the non-biodegradable straws FTIR spectra

each showed the main alkane and alkene groups, with strong peaks in the 2800-3000 cm^{-1} range and 1450 cm^{-1} corresponding to C-H and CH_2 stretching and bending. For PP, there is a sharp peak at 1375 cm^{-1} corresponding to the methyl group which is not present in PE. The PS spectra showed weak aromatic C-H peaks in the range of 2800-3000 cm^{-1}, medium aromatic C=C peaks in the range of 1400-1600 cm^{-1}, and strong =C-H bending peaks in the range of 675-1000 cm^{-1}. For the compostable straw spectra, strong C-H bending peaks were observed in the 675-1000 cm^{-1} range. Additionally, strong peaks near 1750 cm^{-1} and 1200 cm^{-1} were seen, corresponding to a carbonyl and C-O stretches, respectively.

The PE, PP, PS and the non-biodegradable straws spectra showed small peaks in the 1540-1800 cm^{-1}, corresponding to the formation of the carbonyl by substitution of a hydrogen atom with an oxygen atom. The carbonyl index (CI) was calculated for PE, PP, PS, and non-biodegradable straws, corresponding to the degree of photodegradation (Table 2). Carbonyl index is defined as the ratio of the absorbances of the carbonyl band maximum and reference band; therefore, the larger the carbonyl index, the more degradation that occurred. The carbonyl index of the compostable straws could not be accurately determined due to the carbonyl and C-O stretches already found in the plastic.

For all plastic samples, there was a significant increase in content of carbonyl groups due to natural weathering. Barbeş et al. observed a carbonyl index of 0.600 after 160 days of degradation of additive-free PP[23], and Mylläri et al. recorded a carbonyl index of 0.300 after 85 days of degradation of additive-free PS[18]. Extrapolation of their curves to 365 days yields carbonyl indices of 1.73 and 1.63, respectively. As ageing time increased, PS was oxidized at much higher rate than PE and PP, and after one year of UV exposure, PS showed the most visual signs of degradation as well as had the highest carbonyl index. PS degrades faster than PP and PE because the nature of the aromatic bonds of the ring-based backbone. These bonds absorb certain frequencies of light that promote electrons to higher energy anti-bonding orbitals that can break bonds[24]. The non-biodegradable straws likely have more stabilizers than the raw PP, hence its carbonyl index is lower.

GCMS Results

The degradation products of PS, PP, and PE in the saltwater were extracted in hexane and analyzed using GCMS (Table 3). The retention times were recorded for each peak in the spectra and compounds were identified using a library search. The degradation products for the compostable and non-biodegradable straws were below the limit of detection and therefore not quantifiable.

As seen in Table 3, the degradation products of PE and PP are aliphatic hydrocarbons whereas the degradation of PS results in cyclic aromatic compounds. In literature, other compounds have been observed after thermal degradation in an oxidative environment[6,25] that might also be expected degradation products in this study. For example, Singh et al. reported that methane, ethane, styrene, toluene, and ethylbenzene were the dominant gases during thermal degradation in an oxidative environment of PS, PP, and PE[25]. There are several reasons we believe the compounds in Table 3 are only a partial list of possible degradation products for these samples. In an oxidative atmosphere, like the artificial seawater environment in this study, it is expected that the relative contents of aliphatic hydrocarbons and aromatic hydrocarbons are dramatically reduced due to an oxygen atom attack. Additionally, due to the high injection temperature of 350°C and column temperature of 60°C selected to ensure all degradation compounds could be observed, there may have been a loss of carbonyl bonds at the ends of degradation products. Therefore, plausible additional degradation products may include the oxygenated forms of those found in Table 3. Benzoic acid is stable at temperatures upwards of 450°C and therefore was unaffected by the high temperature GCMS.

The products identified using this method were relatively long chain alkenes yet shorter chain alkene compounds are expected based on the literature. For example, degradation products observed by Qin *et al*., include highly volatile compounds, such as ethyne, ethylene, and propylene[6]. While those compounds were not observed in this study, we believe this could be a factor of the experimental setup. Though the shaker table was set to 25°C, the UV lamp that was placed above the samples operates at 70°C, thereby heating the environment and could have caused some of the shorter chain components to evaporate leaving the longer chain components behind. Based on the lack of observable short-chain components, we cannot definitively conclude whether or not chain scission has occurred among these samples. Future work could include molecular weight determination of the samples to better understand if chain scission is at play. Regardless of the limitations of this study, it is essential to be able to identify these types of compounds. This is supported by a study by Wang et al., who found further reactions repolymerize monomers and oligomers produced from chain scission degradation into nanoplastics and microplastics[26]. GCMS methods to detect small molecule gasses during thermal degradation have been reported, but characterization of these larger molecules using this method is novel as far as the authors are aware.

Table 2: Carbonyl index of the PE, PP, PS, and non-biodegradable straws

Plastic Type	Carbonyl Index
PE	1.81
PP	1.88
PS	1.93
Non-biodegradable straws	1.83

Conclusions

This study applied established and novel characterization

Table 3: Summary of degradation compounds with their specific fragment ions and average values

Plastic Type	Fragment Ion	RT (min)	m/z
Baseline	Hexane	2.782	57
PS	Styrene	7.017	104
	Benzoic Acid	14.789	105
PP	2,4-Dimethyl-1-heptene	5.842	70
	2,4,6-Trimethyl-1-nonene	12.522	69
	2,4,6,8-Tetramethyl-10-undecene	19.167	69
PE	1-Undecene	12.458	154
	1-Dodecene	15.292	168
	1-Tridecene	18.167	182

methods for analyzing common consumer plastics and their degradation compounds after exposure to ultraviolet light and physical mixing in a simulated ocean environment. An original technique was developed and employed to extract and identify dilute organic compounds from the surrounding saltwater solution. The change in yellowness index of all samples, ranging from 11 ± 3 to 36 ± 9, suggests photooxidation is taking place. The digital imaging method allows for measurement and analysis of the color of plastic pellets that are adequate for analyzing general trends in degradation. The FTIR results show formation of carbonyl groups in all exposed samples with carbonyl indices ranging from 1.81 to 1.93. After one year of UV exposure, PS showed the most visible signs of degradation as well as had the highest carbonyl index. SEM images show clear indentations and surface smoothening of all samples. The degradation products identified by GCMS are aliphatic hydrocarbons for PE and PP, whereas the degradation of PS results in cyclic aromatic compounds. This novel GCMS protocol identifies large-molecule organic degradation products, overcoming obstacles associated with other methods due to its low limit of detection. Because these large molecules have the potential to repolymerize to nanoplastics and microplastics, this procedure may be useful in understanding the ultimate fate of plastics in marine environments. This information could ultimately be used in the development of plastic pollution removal methods as well as protocols for preventing plastic pollutants from entering oceanic environments. These practices could ultimately reduce or eliminate the negative effects of plastic pollutants in oceanic environments.

Acknowledgements

The authors thank the Independent Project/ Research Opportunities Program and Chemical Engineering Department at Rose-Hulman Institute of Technology for funding this project. We also thank Mr. Frank Cunning of the Chemical Engineering Department and Mr. Lou Johnson and Dr. Stephanie Poland of the Chemistry Department for providing access to and training on equipment. The authors also thank Dr. Jared Tatum at Ampacet Corporation for providing the polymer pellets.

References

(1). Jambeck, J. R.; Geyer, R.; Wilcox, C.; Siegler, T. R.; Perryman, M.; Andrady, A.; Narayan, R.; Law, K. L. *Science* **2015**, *347*, 768–771.
(2). Gregory, M. R. *Philos. T. Roy. Soc. B.* **2009**, *364*, 2013–2025.
(3). Law, K. L. *Annu. Rev. Mar, Sci.* **2017**, *9*, 205–229.
(4). Beaumont, N. J.; Aanesen, M.; Austen, M. C.; Börger, T.; Clark, J. R.; Cole, M.; Hooper, T.; Lindeque, P. K.; Pascoe, C.; Wyles, K. J. *Mar. Pollut. Bull.* **2019**, 189–195.
(5). Syranidou, E.; Karkanorachaki, K.; Amorotti, F.; Avgeropoulos, A.; Kolvenbach, B.; Zhou, N.-Y.; Fava, F.; Corvini, P. F.-X.; Kalogerakis, N. *J. Hazard. Mater.* **2019**, *375*, 33–42.
(6). Qin, L.; Han, J.; Zhao, B.; Wang, Y.; Chen, W.; Xing, F. *J. Anal. Appl. Pyrol.* **2018**, *136*, 132–145.
(7). Goldstein, M. C.; Titmus, A. J.; Ford, M. *PLOS ONE* **2013**, *8*, e80020.
(8). El Hadri, H.; Gigault, J.; Maxit, B.; Grassl, B.; Reynaud, S. *NanoImpact* **2020**, *17*, 100206.
(9). Cai, L.; Wang, J.; Peng, J.;, Wu, Z.; Tan, X.; *Sci. Total Environ.* **2018**, *628–629*, 740-747.
(10). Song, Y. K.; Hong, S. H.; Jang, M.; Han, G. M.; Jung, S. W.; Shim, W. J.; *Environ. Sci. Technol.* **2017**, *51*, 4368–4376.
(11). Gewert, B.; Plassmann, M.; Sandblom, O.; MacLeod, M. *Environ. Sci. Technol. Lett.* **2018**, *5*, 272–276.
(12). Duemichen, E.; Eisentraut, P.; Celina, M.; Braun, U. *J. Chrom. A* **2019**, *1592*, 133–142.
(13). Erni-Cassola, G.; Zadjelovic, V.; Gibson, M. I.; Christie-Oleza, J. A. *J. Hazard. Mater.* **2019**, *369*, 691–698.
(14). Serway, R. A.; Beichner, R. J.; Jewett, J. W. *Physics for Scientists and Engineers*, 5th ed., Saunders College Publishing, Philadelphia, PA, USA **2000**.
(15). Dissanayake, T. M. R.; Amarathunga, K. S. P.; Thilakaratne, B. M. K. S.; Bandara, D. M. S. P.; Fernando, A. J. *Tropical Agricultural Research* **2015**, *26*, 707.
(16). Yam, K. L.; Papadakis, S. E. A Simple Digital Imaging Method for Measuring and Analyzing Color of Food Surfaces. *J. Food Eng.* **2004**, *61*, 137–142.
(17). Lindbloom, B. J. RGB Working Space Information http://www.brucelindbloom.com/index.html?WorkingSpaceInfo.html.
(18). Mylläri, V.; Ruoko, T.-P.; Syrjälä, S. *J. Appl. Polym. Sci.* **2015**, *132*, 42246.
(19). Yousif, E.; Haddad, R. *Springerplus* **2013**, *2*.
(20). Callister, W. D.; Rethwisch, D. G. *Fundamentals of Materials Science and Engineering: An Integrated Approach*, 5th ed. John Wiley & Sons, Hoboken, NJ, USA **2005**.
(21). León, K.; Mery, D.; Pedreschi, F.; León, J.; *Food Res. Int.* **2006**, *39*, 1084-1091.
(22). Segura, L.I.; Salvadori, V.O.; Goñi, S.M.; *Int. J. Food Prop.* **2017**, 20, S467-S477.
(23). Barbeş, L.; Rădulescu, C.; Stihi, C. *Rom. Rep. Phys.* **2014**,*66*, 765–777.
(24). Giron, N. H.; Celina, M. C. *Polym. Degrad. Stabil.* **2017**, *145*, 93–101.
(25). Singh, R. K.; Ruj, B.; Sadhukhan, A. K.; Gupta, P. *J. Energy Inst.* **2020**, *93*, 1020–1035.
(26). Wang, J.; Tan, Z.; Peng, J.; Qiu, Q.; Li, M. *Mar. Environ. Res.* **2015**, *113*, 7-17.